JVI Journals.ASM.org

Severe Acute Respiratory Syndrome-Associated Coronavirus Vaccines Formulated with Delta Inulin Adjuvants Provide Enhanced Protection while Ameliorating Lung Eosinophilic Immunopathology

Yoshikazu Honda-Okubo,[a] Dale Barnard,[b] Chun Hao Ong,[a] Bi-Hung Peng,[c] Chien-Te Kent Tseng,[c] Nikolai Petrovsky[a,d]

Vaxine Pty Ltd., Adelaide, Australia[a]; Institute for Antiviral Research Utah State University, Logan, Utah, USA[b]; University of Texas Medical Branch, Galveston, Texas, USA[c]; Department of Diabetes and Endocrinology, Flinders University, Adelaide, Australia[d]

ABSTRACT

Although the severe acute respiratory syndrome-associated coronavirus (SARS-CoV) epidemic was controlled by nonvaccine measures, coronaviruses remain a major threat to human health. The design of optimal coronavirus vaccines therefore remains a priority. Such vaccines present major challenges: coronavirus immunity often wanes rapidly, individuals needing to be protected include the elderly, and vaccines may exacerbate rather than prevent coronavirus lung immunopathology. To address these issues, we compared in a murine model a range of recombinant spike protein or inactivated whole-virus vaccine candidates alone or adjuvanted with either alum, CpG, or Advax, a new delta inulin-based polysaccharide adjuvant. While all vaccines protected against lethal infection, addition of adjuvant significantly increased serum neutralizing-antibody titers and reduced lung virus titers on day 3 postchallenge. Whereas unadjuvanted or alum-formulated vaccines were associated with significantly increased lung eosinophilic immunopathology on day 6 postchallenge, this was not seen in mice immunized with vaccines formulated with delta inulin adjuvant. Protection against eosinophilic immunopathology by vaccines containing delta inulin adjuvants correlated better with enhanced T-cell gamma interferon (IFN-γ) recall responses rather than reduced interleukin-4 (IL-4) responses, suggesting that immunopathology predominantly reflects an inadequate vaccine-induced Th1 response. This study highlights the critical importance for development of effective and safe coronavirus vaccines of selection of adjuvants based on the ability to induce durable IFN-γ responses.

IMPORTANCE

Coronaviruses such as SARS-CoV and Middle East respiratory syndrome-associated coronavirus (MERS-CoV) cause high case fatality rates and remain major human public health threats, creating a need for effective vaccines. While coronavirus antigens that induce protective neutralizing antibodies have been identified, coronavirus vaccines present a unique problem in that immunized individuals when infected by virus can develop lung eosinophilic pathology, a problem that is further exacerbated by the formulation of SARS-CoV vaccines with alum adjuvants. This study shows that formulation of SARS-CoV spike protein or inactivated whole-virus vaccines with novel delta inulin-based polysaccharide adjuvants enhances neutralizing-antibody titers and protection against clinical disease but at the same time also protects against development of lung eosinophilic immunopathology. It also shows that immunity achieved with delta inulin adjuvants is long-lived, thereby overcoming the natural tendency for rapidly waning coronavirus immunity. Thus, delta inulin adjuvants may offer a unique ability to develop safer and more effective coronavirus vaccines.

The severe acute respiratory syndrome-associated coronavirus (SARS-CoV) was identified in 2003 when a series of fatal pneumonia cases started in Hong Kong (1, 2). SARS-CoV lung infection is characterized by a marked inflammatory cell infiltrate with diffuse alveolar damage (3). Before the disease was controlled by quarantine measures, ~8,000 humans were clinically infected, with an overall case fatality rate of ~10% but with mortality of ~50% in those over 65 years of age (4). After recovery from coronavirus infections, previously infected individuals may be susceptible to reinfection (5, 6). In fact, individuals with waning immunity may be at risk of even more severe disease upon coronavirus reexposure (7). Given the risk of future human outbreaks of SARS-CoV, Middle East respiratory syndrome-associated coronavirus (MERS-CoV) (8), or other coronaviruses, development of an optimal vaccine platform is an ongoing priority.

SARS-CoV is a positive-stranded RNA virus 29.7 kb in length with approximately 14 open reading frames (9). The first SARS-CoV vaccine candidates were produced from inactivated SARS-CoV. Inactivated whole virus (IWV) without adjuvant provided only modest protection, inducing low neutralizing-antibody titers and earlier lung clearance in challenged ferrets (10). In mice, IWV vaccines alone or formulated with alum adjuvant provided partial protection, but this was associated with severe eosinophilic lung

Received 13 October 2014 Accepted 5 December 2014

Accepted manuscript posted online 17 December 2014

Citation Honda-Okubo Y, Barnard D, Ong CH, Peng B-H, Tseng C-TK, Petrovsky N. 2015. Severe acute respiratory syndrome-associated coronavirus vaccines formulated with delta inulin adjuvants provide enhanced protection while ameliorating lung eosinophilic immunopathology. J Virol 89:2995–3007. doi:10.1128/JVI.02980-14.

Editor: S. Perlman

Address correspondence to Nikolai Petrovsky, nikolai.petrovsky@flinders.edu.au.

doi:10.1128/JVI.02980-14

pathology (11–14), similar to the pathology seen with SARS-CoV rechallenges after primary infection (15). It is not known if immunized human subjects might similarly be predisposed to lung immunopathology upon SARS-CoV infection. Another challenge for inactivated SARS-CoV vaccines is the need for biosafety level 3 (BSL3) facilities for vaccine manufacture. An alternative vaccine antigen is the SARS-CoV spike protein (SP), which mediates target cell entry via attachment to angiotensin-converting enzyme 2 and CD209L, leading to receptor-mediated endocytosis (16, 17). While immunization with recombinant SP (rSP) induced protection (18, 19), it similarly exacerbated lung eosinophilic immunopathology, and like with IWV vaccine, this was exacerbated by formulation with alum adjuvant (11, 14). Respiratory syncytial virus (RSV) vaccines formulated with alum similarly caused lung eosinophilic immunopathology and increased mortality when immunized children became infected with RSV (20), suggesting that this is a generalized problem of Th2-polarizing alum adjuvants. There is a critical need, therefore, to identify suitable coronavirus vaccine adjuvants that do not exacerbate, or ideally suppress, virus-induced lung immunopathology. Advax belongs to the class of polysaccharide adjuvants (21, 22) and is based on particles of β-D-[2-1]poly(fructo-furanosyl)α-D-glucose (delta inulin) (23). Delta inulin has been shown to enhance humoral and cellular immunity with a wide variety of vaccines against viruses, including influenza virus (24, 25), Japanese encephalitis and West Nile viruses (26, 27), hepatitis B virus (28), and HIV (29). It induces balanced Th1 and Th2 immune responses (25, 28), which contrasts with alum's marked Th2 bias. Delta inulin is notable for its lack of reactogenicity as demonstrated in human influenza and hepatitis B vaccine trials (30, 31).

This study asked whether given its balanced effects on Th1 and Th2 T-cell immunity, the Advax delta inulin adjuvant platform could be used to enhance SARS-CoV vaccine protection while avoiding the risk of lung eosinophilic immunopathology. As shown below, delta inulin adjuvants successfully enhanced humoral and cellular immunity and protection against SARS-CoV while avoiding the lung immunopathology induced by alum adjuvant.

MATERIALS AND METHODS

Reagents. Recombinant spike protein (rSP) produced in insect cells (BEI catalog no. NR-722; Protein Sciences Corp., Meriden, CT) and Vero cell formaldehyde- and UV light-inactivated whole-virion SARS-CoV (BEI catalog no. NR-3882, lot 480405CA) were both obtained from BEI Resources, NIAID, NIH (Manassas, VA). CpG2006 was purchased from GeneWorks (Adelaide, Australia). Advax adjuvants were supplied by Vaxine Pty Ltd., Adelaide, Australia, with Advax-1 being a preservative-free sterile suspension of delta inulin microparticles at 50 mg/ml in a bicarbonate buffer, whereas Advax-2 additionally included 10 μg CpG per 1 mg delta inulin. Both formulations of Advax adjuvant were used at a standardized dose of 1 mg delta inulin per mouse. Advax adjuvant was formulated with antigen by simple admixture immediately prior to immunization.

Animals. Vaccine immunogenicity studies were performed in accordance with the Animal Experimentation Guidelines of the National Health and Medical Research Council of Australia, approved by the Flinders Animal Welfare Committee, and performed on adult female BALB/c mice 6 to 8 weeks of age as supplied by the Flinders University animal facility. Mice were immunized twice 3 weeks apart with a variety of different vaccine formulations and then bled regularly for 12 months to monitor changes in antibody levels.

The SARS challenge study was conducted in accordance with and with the approval of the Institutional Animal Care and Use Committee of Utah State University. The work was done in the AAALAC-accredited Laboratory Animal Research Center of Utah State University in accordance with the National Institutes of Health Guide for the Care and Use of Laboratory Animals (2010 revision). Female 4- to 6-week-old BALB/c mice weighing 18 to 20 g were obtained from Charles River Laboratories (Wilmington, MA). They were maintained on Wayne Lab Blox and tap water *ad libitum*. At days 3 and 6 after virus challenge, 5 mice from each immunized and control group were sacrificed and the lungs harvested for gross pathology (lung score), lung weights, lung virus titers, and measurement of anti-SARS IgG in lung homogenate.

SARS-CoV. Mouse-adapted SARS-CoV was used throughout the study. The virus used for the challenge study was passaged 25 times through BALB/c mice and was verified as SARS-CoV by enzyme-linked immunosorbent assay ELISA and PCR (2). The virus was sent for sequencing and identified as a SARS-CoV variant as described elsewhere (32).

Serology. SARS-specific antibodies were determined by ELISA. rSP was absorbed to ELISA plates in 0.1 M sodium hydrogen carbonate buffer, pH 9.6, and incubated overnight at 4°C. After blocking with 1% bovine serum albumin-phosphate-buffered saline (BSA-PBS) for 1 h, serum samples diluted in 1% BSA-PBS were incubated for 2 h at room temperature (RT) and washed, and then 100 μl biotinylated anti-mouse IgG, IgG1, IgG2a, IgG2b, IgG3, or IgM antibodies (Abcam) with streptavidin-horseradish peroxidase (HRP) (BD Biosciences) was incubated for 1 h at RT and then incubated with 100 μl of tetramethylbenzidine (TMB) substrate for 10 min; the reaction was then stopped with 1 M phosphoric acid. The optical density at 450 nm (OD_{450}) was measured with a VersaMax ELISA microplate reader (Molecular Devices, CA, USA) and analyzed using SoftMax Pro software.

T-cell assays. Mice were killed by cervical dislocation, and bones and spleens were collected. Bone marrow was isolated from femurs by flushing with 3% fetal bovine serum (FBS)-PBS. Cells were released by pressing against a tea strainer with a rubber syringe plunger, and red blood cells (RBCs) were removed by osmotic shock. Cells were washed with 3% FBS-PBS and then resuspended in RPMI complete medium with 10% heat-inactivated FBS. Splenocytes were labeled with 5 μM carboxyfluorescein succinimidyl ester (CFSE) (Invitrogen Life Technologies) and cultured in 24-well plates at 10^6 cells/ml/well with 1 μg/ml rSP. After 5 days of incubation at 37°C and 5% CO_2, cells were washed with 0.1% BSA-PBS, treated with anti-mouse CD16/CD32 (BD Biosciences) for 5 min at 4°C, and then stained with anti-mouse CD4-allophycocyanin (APC) and anti-mouse CD8a-phycoerythrin (PE)-Cy7 (BD) for 30 min at 4°C. Cells were washed and then analyzed by fluorescence-activated cell sorting (FACS) (FACSCanto II; BD Biosciences) with FACSDiva software. For each lymphocyte subset, proliferation was expressed as the percentage of divided cells (CFSE low) compared to undivided cells (CFSE high). Dot plots representing analysis of 10^5 cells were generated by FlowJo software.

ELISPOT assays. The frequency of antigen-specific antibody- or cytokine-secreting cells was analyzed using biotinylated anti-mouse IgG, IgG1, IgG2a, or IgM antibodies (Abcam), anti-mouse gamma interferon (IFN-γ), interleukin-2 (IL-2), or IL-4 antibody pairs (BD), or LEAF anti-mouse IL-17A and biotin-anti-mouse IL-17A antibody (BioLegend, USA) with streptavidin-HRP (BD Biosciences), according to the manufacturer's instructions. Briefly, single-cell suspensions were prepared from bone marrow and spleens of mice at the indicated time points and plated at 2×10^5 cells/well in 96-well plates precoated with rSP (for antibody detection) or anti-mouse cytokine monoclonal antibody (MAb) (for cytokine detection) overnight at 4°C and then blocked with RPMI–10% FBS. For cytokine assays, the cells were incubated with rSP (10 μg/ml) at 37°C and 5% CO_2 for 2 days. Wells were washed, incubated with biotinylated anti-mouse Ig or anti-mouse cytokine MAb at RT for 2 h, and washed again, and then streptavidin-HRP was added and left for 1 h before washing and addition of aminoethylcarbazole (AEC) substrate solutions (BD Biosciences). Spots were counted with an ImmunoSpot S6 enzyme-linked im-

munosorbent spot (ELISPOT) analyzer (CTL, USA) and analyzed using ImmunoSpot software. The number of spots in negative-control wells was subtracted from the number of spots in SP wells, and the results were expressed as antibody-secreting cells (ASC) per 10^6 bone marrow cells or spots per 10^6 splenocytes.

Lung studies. Immunized and vehicle-treated mice were sacrificed at days 3 and 6 after virus challenge, and lungs were removed. Formalin-fixed lungs were mounted in paraffin blocks. Paraffin-embedded lung sections were stained with hematoxylin and eosin (H&E) and a rat monoclonal antibody (Clone MT-14.7) to eosinophil major basic protein (MBP) (Lee Laboratory, Mayo Clinic, AZ) following a standard immunohistochemistry (IHC) procedure. Diaminobenzidine (DAB) chromogen was used to identify eosinophils as brown-stained cells, as previously described (14). Eosinophil infiltration was scored without knowing animal identity using H&E-stained slides. An overall infiltration score (0 to 3) was assigned to each section according to the amounts of eosinophils in the parenchyma and their distributions through the lung, as follows: 0, no to a few eosinophils; 1, mild eosinophil infiltration; 2, moderate infiltration; and 3, severe infiltration. For confirmation, immunohistochemistry to the eosinophil major basic protein was determined in sections with the highest score of each treatment group.

Statistical analysis. Group comparisons for antibody and ELISPOT tests were done by the Mann-Whitney test. Virus titers were compared using analysis of variance to determine experimental significance, followed by Newman-Keuls pairwise-comparison tests. Survival analysis was done using the Kaplan-Meier method and a log rank test. Pairwise comparisons of survivor curves were analyzed by the Mantel-Cox log rank test, and the relative significance was adjusted to a Bonferroni-corrected significance threshold for the number of treatment comparisons done. Significance is indicated in the figures as follows: *, $P < 0.05$; **, $P < 0.01$; ***, $P < 0.005$; and ****, $P < 0.001$.

RESULTS

Vaccine effects on humoral immunity. To assess the ability of Advax adjuvant formulations to enhance the immunogenicity of recombinant spike protein (rSP), adult female BALB/c mice ($n = 6$/group) were given two intramuscular (i.m.) immunizations 3 weeks apart of 1 μg rSP alone or formulated with Advax-1 or -2 or CpG adjuvant. Formulation with Advax-1 or -2 significantly enhanced SP-specific immunoglobulin responses compared to immunization with antigen alone. Advax-1 significantly enhanced the IgG1 response at 2 weeks postboost, which was maintained out to 1 year postimmunization (Fig. 1A). In contrast, Advax-2 significantly increased a broad range of antibody isotypes, namely, IgG1, IgG2a, IgG2b, and IgG3, with this pattern being maintained for 1 year postimmunization. CpG adjuvant significantly increased SP-specific IgG2a, IgG2b, and IgG3 but not IgG1 at 2 weeks postimmunization, with this pattern maintained for 1 year postimmunization. SP-specific IgM responses peaked at 2 weeks postimmunization in all groups, but interestingly, they remained significantly higher in both Advax-adjuvanted groups than in the group receiving unadjuvanted rSP alone out to 1 year postimmunization, suggesting the generation of long-lived memory IgM-positive B cells in the Advax-immunized groups. The serological response patterns induced by the different adjuvants were largely mirrored by the frequency of isotype-specific antibody-secreting cells (ASC) in the bone marrow of immunized mice. Advax-1 was exclusively associated with IgG1-positive ASC, whereas Advax-2 was associated with both IgG1- and IgG2a-positive ASC (Fig. 1B). There were 2- to 3-fold more IgM-positive ASC in the Advax-immunized mice at 1 year postimmunization.

SP-specific serum immunoglobulin levels were relatively stable out to 1 year postimmunization, except in the CpG adjuvant group, in which an accelerated decline in total IgG and IgG1 levels was seen starting at ~12 weeks postimmunization (Fig. 1C). At 1 year postimmunization, serum IgG1 levels in the CpG-adjuvanted group were significantly lower than those in all other groups, including the group given unadjuvanted rSP alone. A similar pattern emerged for serum IgG2a and IgG2b levels, with the CpG group showing a fast decay starting at ~12 weeks. IgG2a and IgG2b levels in the Advax-2 group showed a minimal decline out to 1 year postimmunization.

Vaccine effects on T-cell immunity. To assess effects on short- and long-term T-cell immunity, SP-specific CD4 and CD8 T-cell proliferation was measured by CFSE assay on splenocytes obtained 2 weeks or 1 year postimmunization. At 2 weeks postimmunization, there were no significant differences between groups in rSP-stimulated CD4 or CD8 T-cell proliferation (Fig. 2A). However, at 1 year postimmunization, the Advax-1 group had significantly higher SP-specific CD4 and CD8 T-cell proliferation than all the other vaccine groups. Interestingly, the CpG group showed a consistent trend to reduced SP-specific CD4 and CD8 T-cell proliferation even compared to the group receiving unadjuvanted rSP alone, as highlighted in the representative FACS CFSE profiles shown in Fig. 2C.

The frequency of T cells secreting Th1, Th2, or Th17 cytokines in response to rSP stimulation was measured by cytokine ELISPOT assay. The frequency of IFN-γ-secreting T cells at 2 weeks postimmunization was significantly higher in the Advax-2 than in the other groups and was also significantly increased in the Advax-1 and CpG groups to a degree similar to that for the group given unadjuvanted rSP alone (Fig. 2B). Interestingly, at 1 year postimmunization, the Advax-1 group now demonstrated the highest frequency of IFN-γ-secreting T cells, with the frequency in the Advax-2 group having fallen back to the level in the unadjuvanted rSP group and that in the CpG group having fallen significantly below that in the unadjuvanted rSP group. This indicates that whereas CpG adjuvant induced a short-lived population of IFN-γ-secreting T cells, Advax-1 induced a long-lived population of such cells. The pattern of IL-2-secreting T cells was similar to that for IFN-γ, being significantly higher in the Advax-1 group than in the unadjuvanted rSP group at both 2 weeks and 1 year postimmunization and significantly lower in the CpG group than in the unadjuvanted rSP group at 1 year postimmunization.

IL-4 is the major cytokine produced by Th2 cells. Consistent with the significant enhancement of serum IgG1 (a Th2 isotype) by Advax-1, this group showed a significantly higher frequency of IL-4-secreting T cells at both 2 weeks and 1 year postimmunization than the other groups. Consistent with its known Th1 bias (33), the CpG group showed almost complete absence of IL-4-secreting T cells at both 2 weeks and 1 year postimmunization. A similar although less marked trend was seen in the Advax-2 group.

The frequency of IL-17-secreting cells, a marker of Th17 cells, was very low, at about 1/10 the frequency of the other T-cell subsets. Nevertheless, IL-17-secreting T cells were significantly increased in both the Advax-1 and -2 groups at 2 weeks postimmunization, although only in the Advax-2 group at 1 year postimmunization.

To determine whether the IFN-γ ELISPOT responses represented CD4 or CD8 T cells, splenocytes of immunized animals were stimulated with SP-specific peptides representing known BALB/c CD4 and CD8 T-cell epitopes in an IFN-γ ELISPOT assay. The vast majority of IFN-γ spots were generated in response to the

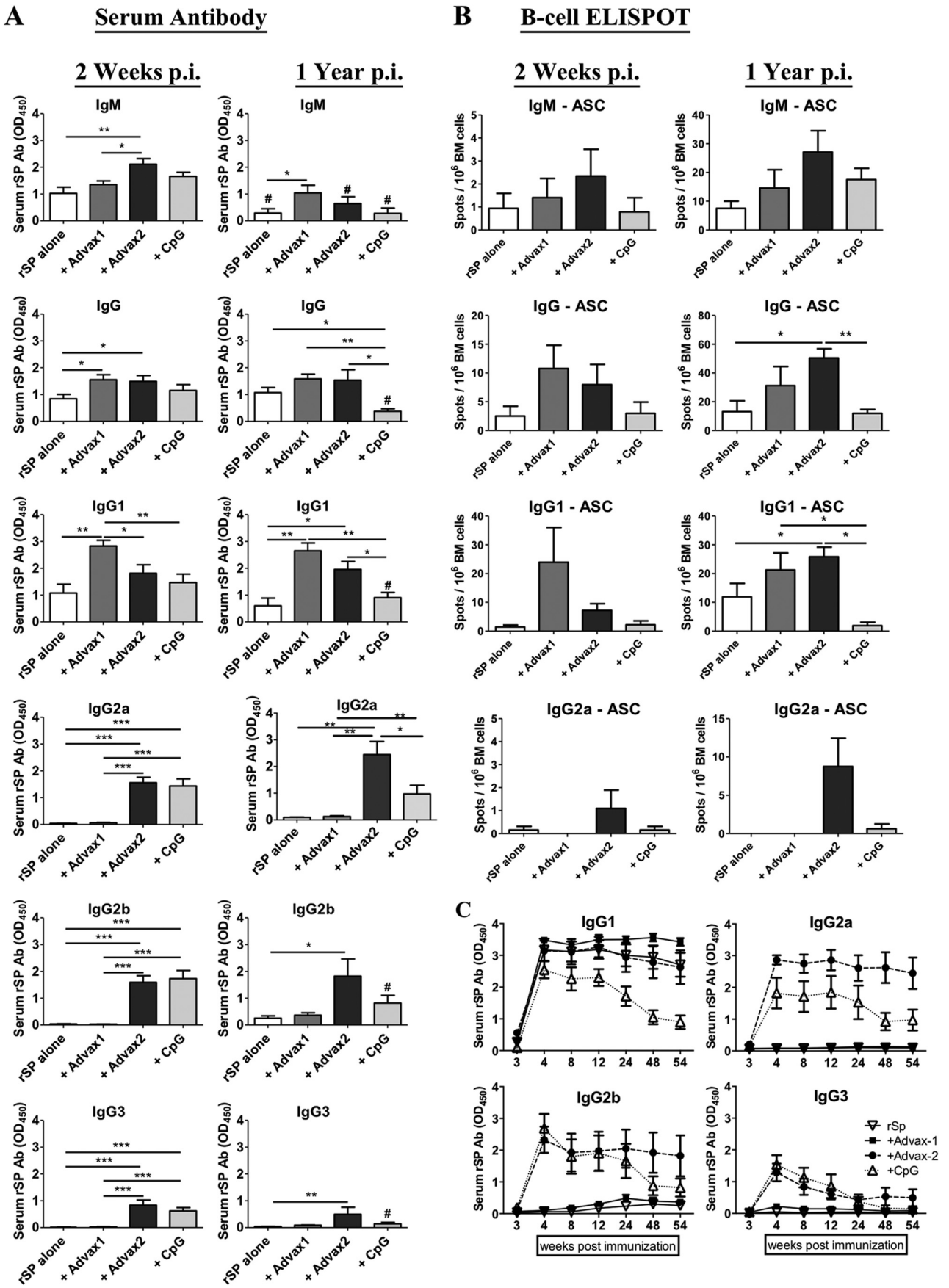
A
Serum Antibody
2 Weeks p.i.
1 Year p.i.
IgM
IgG
IgG1
IgG2a
IgG2b
IgG3
Serum rSP Ab (OD450)
rSP alone
+ Advax1
+ Advax2
+ CpG
B
B-cell ELISPOT
2 Weeks p.i.
1 Year p.i.
IgM - ASC
IgG - ASC
IgG1 - ASC
IgG2a - ASC
Spots / 10^6 BM cells
C
IgG1
IgG2a
IgG2b
IgG3
rSp
+Advax-1
+Advax-2
+CpG
weeks post immunization

CD4 peptide, with just a few spots detected in the CD8 peptide wells (Fig. 2D), consistent with most of the IFN-γ responses coming from SP-specific CD4 T cells.

To further explore adjuvant effects on T-cell cytokine phenotype, splenocytes obtained at 2 weeks and 1 year postimmunization were stimulated with rSP and cytokines measured in the supernatants. Reflecting the ELISPOT findings, splenocytes from the Advax-1 group produced significantly higher IFN-γ, IL-2, IL-4, and IL-17, as well as IL-6, IL-10, and tumor necrosis factor alpha (TNF-α), levels (Fig. 3). This indicates an ability of Advax-1 adjuvant to induce long-lived memory T cells producing a broad range of Th1, Th2, and Th17 cytokines. Splenocytes obtained at 2 weeks and 1 year postimmunization from the CpG and, to a lesser extent, Advax-2 groups demonstrated low SP-stimulated IL-2, IL-4, IL-6, and IL-10 secretion even compared to that in the unadjuvanted rSP group. Consistent with the ELISPOT data, at 2 weeks postimmunization the CpG and Advax-2 groups showed significantly increased SP-stimulated IFN-γ production. However, at 1 year postimmunization the CpG group exhibited significantly reduced SP-stimulated IFN-γ production, and that by the Advax-2 group was no longer higher than that by the unadjuvanted rSP group. CpG was also associated with significantly lower SP-stimulated TNF-α production at both 2 weeks and 1 year postimmunization than in the other groups. IL-17 was the only cytokine that was significantly increased in the Advax-2 group at 1 year postimmunization.

Vaccine effects on SARS-CoV protection. When unimmunized mice were challenged with SARS-CoV (V02225) at the 95% lethal dose (LD_{95}), infected animals died between days 4 and 8, with 90 to 100% mortality achieved by day 8 (32). The lungs of these mice were severely inflamed and exhibited extreme lung consolidation. Weight loss was excessive, and the occasional surviving animal lost 20% or more of its weight but then regained it by day 10. Virus titers in the lungs generally exceeded 10^7 PFU/g tissue, with the titers peaking at day 3 to 4 and persisting at least until day 7 in mice that survived.

The primary objective was to assess the ability of the Advax delta inulin adjuvant formulations to enhance vaccine protection. For a comparator, we included an alum adjuvant to reproduce its known propensity to enhance lung immunopathology (14). We also included comparator groups immunized with an inactivated whole-virus (IWV) antigen with or without Advax-2 to see whether any protective adjuvant effects might be generalizable to whole-virus antigens. Control groups received either vehicle or Advax-1 or Advax-2 adjuvant alone to test whether the delta inulin adjuvants had any nonspecific protective effects against coronavirus infection.

All except one mouse that received vehicle alone succumbed to infection, with similar mortality rates in mice injected with Advax-1 or -2 alone, consistent with a lack of nonspecific protection (Fig. 4A). All active vaccine formulations without or with adjuvant significantly protected mice against lethal infection, with the unadjuvanted IWV vaccine being the least protective but still reducing mortality by greater than 90% compared to that of mice injected with vehicle or adjuvant alone.

Vaccine effects on serum IgG titers. Fourteen days after the booster immunization, the group receiving 10 μg rSP plus Advax-2 (rSP 10 μg+Advax-2 group) had the highest serum SARS-specific IgG titers, significantly greater than those in the unadjuvanted IWV group, which had undetectable titers (Fig. 4B). By day 3 postchallenge, IgG titers had risen more than 64-fold in all active vaccine groups but were still undetectable in the vehicle- or adjuvant-alone control groups. By day 3 postchallenge, titers were significantly ($P < 0.05$) higher in the rSP 2.5 μg+Advax-2 group than in the alum-adjuvanted group or the group given 2.5 μg rSP alone (rSP 2.5 μg alone group). By day 6 postchallenge, IgG titers had risen a further ~8-fold in the active vaccine groups and were now detectable in the vehicle control groups. The rSP 2.5 μg+Advax-2 group continued to have the highest titers, which, along with those in the rSP 2.5 μg+Advax-1 group, were significantly higher than those in the rSP 2.5 μg alone group. At day 21 postchallenge, whereas the titers in the previously highest-titer groups (i.e., rSP 2.5 μg+Advax-1 and rSP 2.5 μg+Advax-2) had already fallen from their day 6 postchallenge peak, the highest titers were now seen in the previously lower-titer unadjuvanted rSP and IWV groups, suggesting a longer ongoing viral stimulus to antibody production in these groups.

Vaccine effects on serum SARS-CoV neutralizing-antibody titers. The serum SARS-CoV neutralization assay results largely mirrored the IgG results, with some notable exceptions. No SARS serum neutralizing antibody was detectable prechallenge on day 14 postboost, a time when low but detectable IgG titers were already present in the active vaccine groups. Serum neutralizing antibody first became detectable at day 3 postchallenge in the active vaccine groups except for the IWV-alone group (Fig. 4C) and was significantly higher in the rSP 10 μg+Advax-2 group. On day 6 postchallenge, significantly higher titers were again seen in the rSP 10 μg+Advax-2 group as well as the three adjuvanted 2.5 μg rSP groups compared to the rSP-alone or IWV groups. An interesting feature was that the rSP 10 μg+Advax-2 group had the highest neutralizing-antibody titers at both days 3 and 6 postchallenge, despite not having the highest serum IgG titers (Fig. 4B). The rSP 10 μg alone group exhibited the opposite phenomena, with a high serum IgG (Fig. 4B) but low SARS neutralizing antibody (Fig. 4C) titer. This suggests that some vaccines, notably the rSP 10 μg+Advax-2 formulation, may induce more neutralizing antibody as a percentage of SARS-specific IgG production.

Vaccine effects on lung histology and edema. All active vaccine formulations with or without adjuvant significantly ameliorated the gross lung pathology as measured by histopathology lung scores at days 3 and 6 postchallenge, compared to vehicle or adjuvant-alone controls, with no significant differences between active vaccine groups (Fig. 5A). Lung weight is a useful objective measure of lung edema. Again all active vaccine formulations significantly ameliorated lung edema on day 3 postchallenge, compared to vehicle or adjuvant-alone controls, with no significant

FIG 1 Adjuvant effects on humoral immunity. (A) Female BALB/c mice were immunized i.m. twice with 1 μg rSP alone or with Advax-1, Advax-2, or CpG and then periodically bled for measurement of serum SP-specific antibodies by ELISA. (B) At 2 weeks and 1 year postimmunization, mice ($n = 6$ for each time point) were sacrificed and bone marrow collected for measurement of memory B-cell frequency by ELISPOT assay. (C) Also shown are changes of serum SP-specific IgG titers over time. All values are means ± standard errors of the means (SEM). #, group where there was a significant ($P < 0.05$) fall in antibody titer between 2 weeks and 1 year postimmunization. *, $P < 0.05$; **, $P < 0.01$; ***, $P < 0.005$), ****, $P < 0.001$.

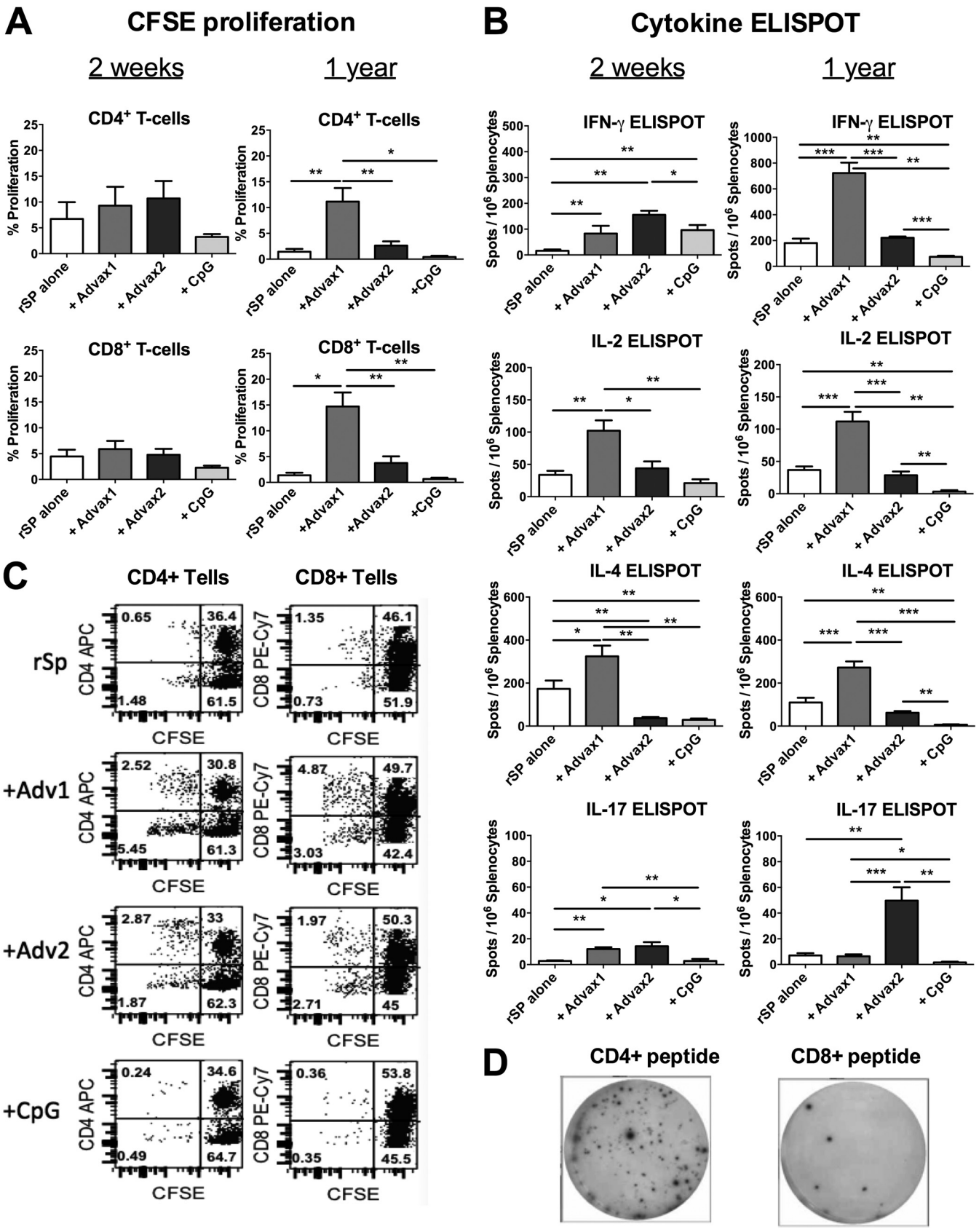

FIG 2 Adjuvant effects on T-cell immunity. (A and B) At 2 weeks and 1 year postimmunization, splenocytes were harvested from immunized mice ($n = 6$ for each time point, divided into 2 groups of 3 mice) for rSP-stimulated T-cell proliferation by CFSE assay (A) and cytokine ELISPOT assays (B). (C) Representative FACS CFSE plot of the data in panel A, demonstrating reduced CD4 and CD8 T-cell proliferation in response to SP in the CpG group. (D) Representative IFN-γ ELISPOT assays showing that the majority of SP-specific IFN-γ producing splenocytes in immunized mice recognize the CD4 epitope peptide from SP (left well) rather than the CD8 epitope peptide. All values are means ± SEM.

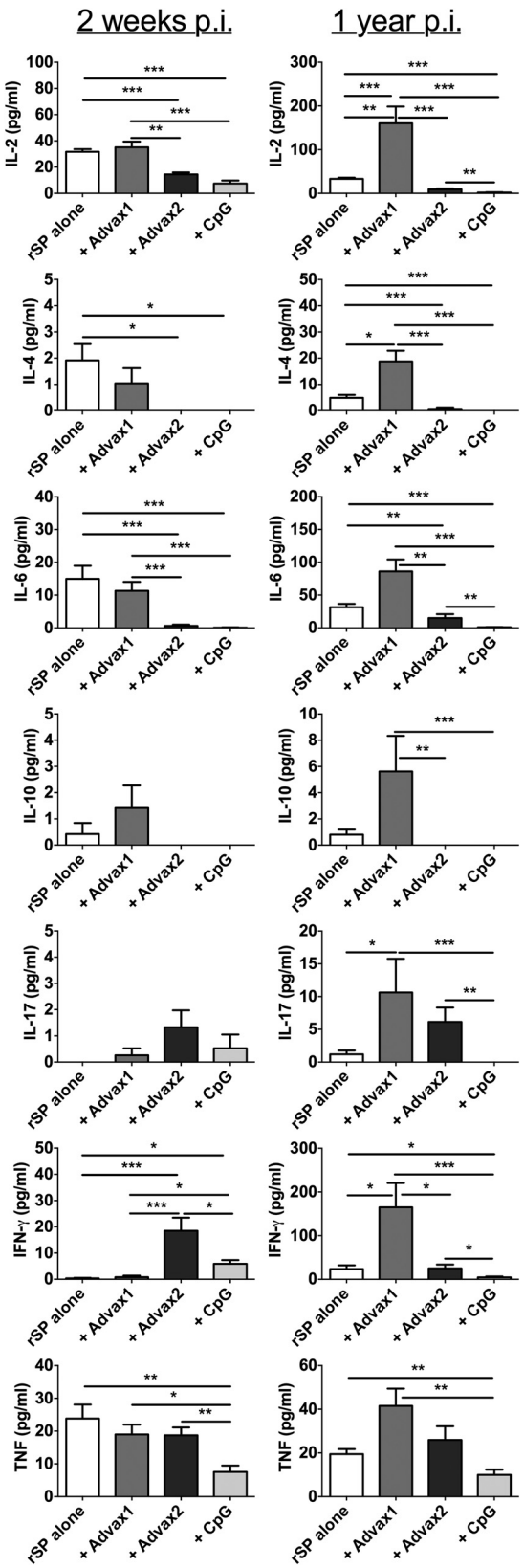

FIG 3 Adjuvant effects on T-cell cytokine responses. Splenocytes were harvested at 2 weeks and 1 year postimmunization and stimulated with rSP for 2 days, and cytokines in the culture supernatants were measured by cytometric bead array (CBA) assay. Values are means ± SEM.

differences between active vaccine groups (Fig. 5C). However, significant differences in lung edema became apparent on day 6 postchallenge, with the lowest lung weights in the groups that received antigen formulated with Advax-1, Advax-2, or alum adjuvant and the highest lung weights in groups that received unadjuvanted rSP or IWV (Fig. 5D).

Vaccine effects on lung virus titers. To assess the ability of the various vaccine formulations to inhibit SARS-CoV replication in the lung, homogenized lung tissue of mice sacrificed at day 3 or 6 postchallenge was assayed for virus. On day 3 postchallenge, all the Advax-adjuvanted vaccine groups plus the alum-adjuvanted group had significantly reduced lung virus titers compared to those in the adjuvant-alone or vehicle control groups (Fig. 5E). In contrast, at day 3 postchallenge, virus titers in mice that received 2.5 μg unadjuvanted rSP or IWV alone were not significantly different from those in vehicle or adjuvant control mice. The lowest mean lung virus titers at day 3 postchallenge were seen in mice that received rSP (either 2.5 or 10 μg) with Advax-2. No major differences in lung virus titers between active vaccine groups were observable on day 6 postchallenge, although the rSP 2.5 or 10 μg plus Advax-2 groups continued to have the lowest virus titer point estimates (Fig. 5F).

Vaccine effects on lung IgG titers. All of the active vaccine formulations resulted in detectable lung SARS-specific IgG titers at days 3 and 6 postchallenge, with significantly lower titers in the rSP 2.5 μg and IWV-alone groups at day 3 postchallenge than in the other active vaccine groups (Fig. 5G). By day 6 postchallenge, the rSP 2.5 μg and IWV-alone groups had caught up, and there were no significant differences between any of the active vaccine groups (Fig. 5H).

Vaccine effects on lung eosinophilic immunopathology. Histology and eosinophil infiltration were assessed blind using H&E-stained lung slides from mice ($n = 5$/group) sacrificed day 6 postchallenge. An eosinophil infiltration score of 0 to 3 was assigned to each section according to the number of eosinophils in the parenchyma and their distribution throughout the lung. Control challenged animals that had been immunized with vehicle or adjuvant alone, despite severe lung pathology with edema, neutrophilic, and histiocytic alveolitis and intra-alveolar fibrin accumulation, demonstrated minimal eosinophil infiltration (Fig. 6). The highest eosinophil infiltration scores were seen in mice immunized with the unadjuvanted vaccines: from highest down, IWV (mean score, 3.0/3), rSP 10 μg (2.6/3), rSP 2.5 μg (1.6/3), and rSP 2.5 μg+alum (1.0/3). Mice immunized with Advax-adjuvanted vaccine had low eosinophil scores: rSP 2.5 μg+Advax-2, score 0.0/3; rSP 10 μg+Advax-2, 0.4/3; IWV+Advax-2, 0.4/3; and rSP 2.5 μg+Advax-1, 0.6/3. For confirmation, immunohistochemistry to eosinophil major basic protein was determined in mice with the highest score from each treatment group. This confirmed severe lung eosinophil infiltration in the unadjuvanted IWV and rSP groups and alum-adjuvanted rSP group (Fig. 6). In contrast, only occasional eosinophils were seen in the lungs of mice immunized with Advax-adjuvanted rSP or IWV.

DISCUSSION

There is an ongoing need for vaccines to avert human coronavirus threats, with MERS-CoV being a current focus of vaccine development efforts (34). In this study, we tested adjuvant and antigen permutations to identify an optimal formulation that would protect against both clinical infection and lung eosinophilic immu-

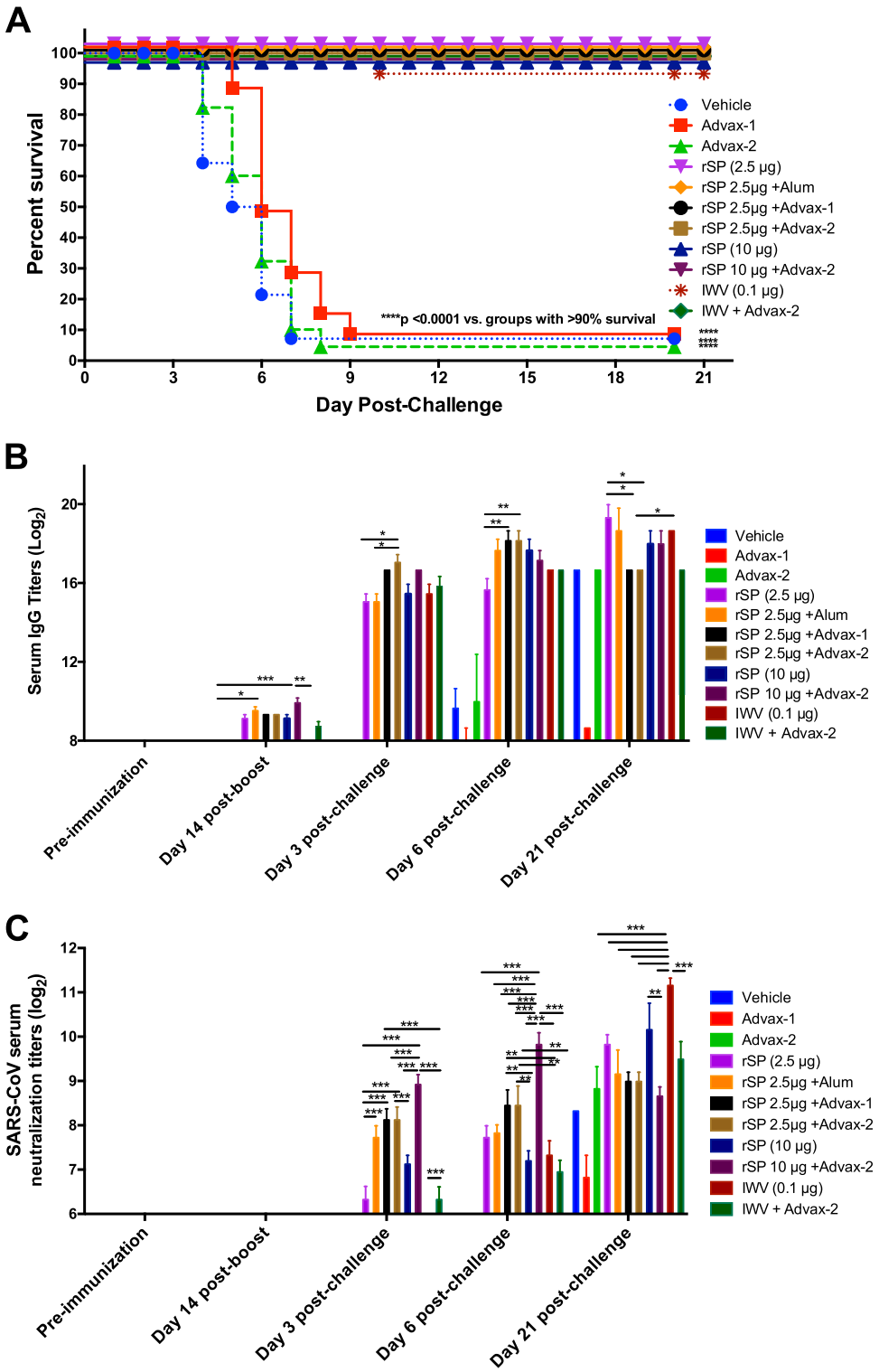

FIG 4 Vaccine protection and serum antibody titers. Groups of mice ($n = 15$) were immunized twice i.m. with vehicle, Advax-1 or -2 adjuvant alone, rSP alone or formulated with alum, Advax-1, or Advax-2, or IWV alone or with Advax-2 and then at 4 weeks postimmunization challenged with SARS-CoV. Shown are survival curves (A), serum SARS-CoV-specific IgG titers (B), and serum SARS-CoV neutralization titers (C). All values are means ± SEM.

nopathology, a problem exacerbated by alum-formulated vaccines (14). All the active vaccine formulations protected against SARS-CoV mortality. The weakest protection was obtained with rSP or IWV alone, as reflected in higher lung virus titers, edema, and eosinophil infiltration. At the other end of the spectrum, mice immunized with rSP plus Advax-2 had the lowest lung virus titers at day 3 postchallenge, together with the highest SARS-CoV neutralization titers and lowest day 6 lung weights. Although rSP for-

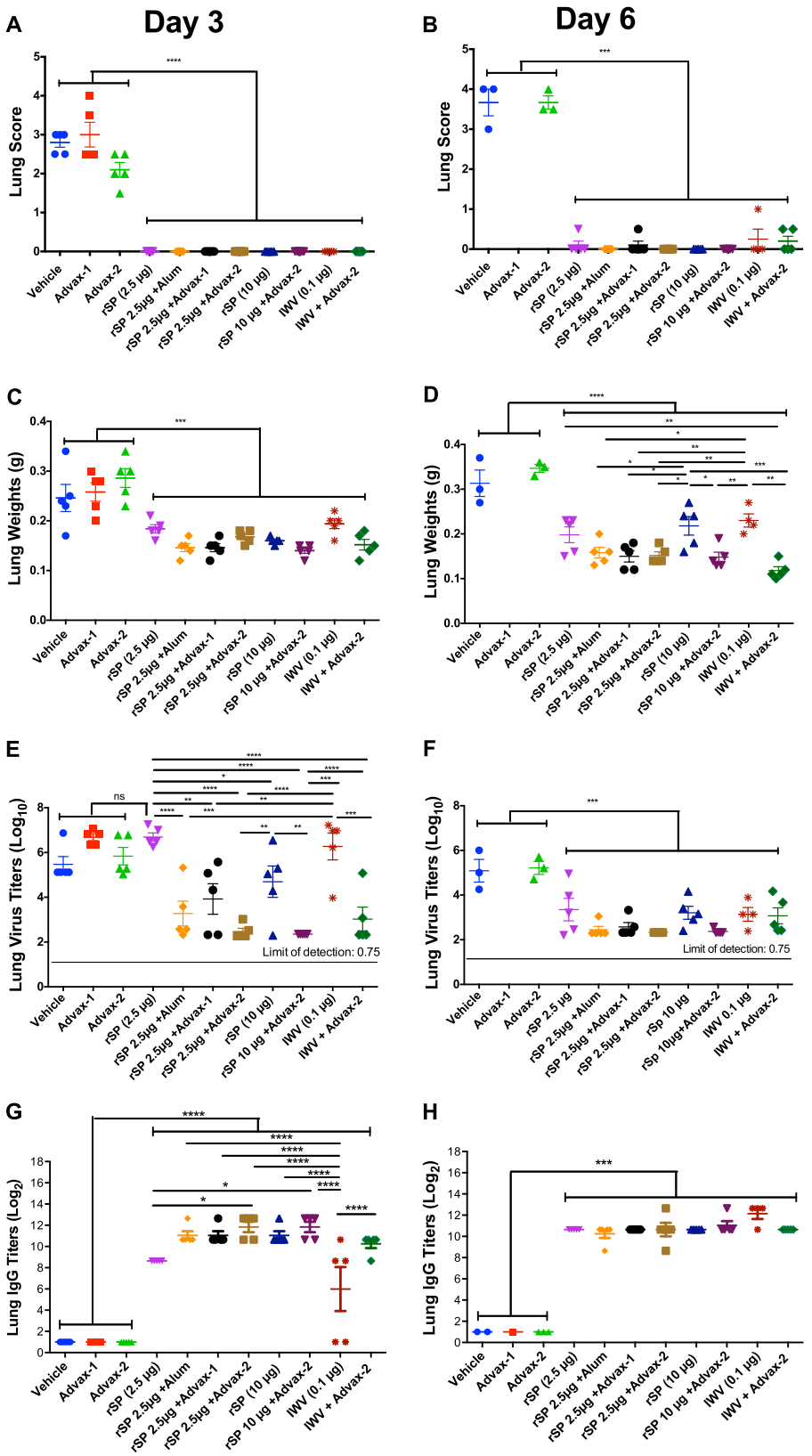

FIG 5 Vaccine effects on SARS-CoV lung pathology and virus titers. Groups of immunized mice ($n = 5$ for each time point) were sacrificed on days 3 and 6 postchallenge and lungs harvested. Shown are lung histology scores (A and B), lung weights (C and D), lung virus titers (limit of detection, 0.75) (E and F), and SP-specific lung IgG titers (G and H). All values are means ± SEM.

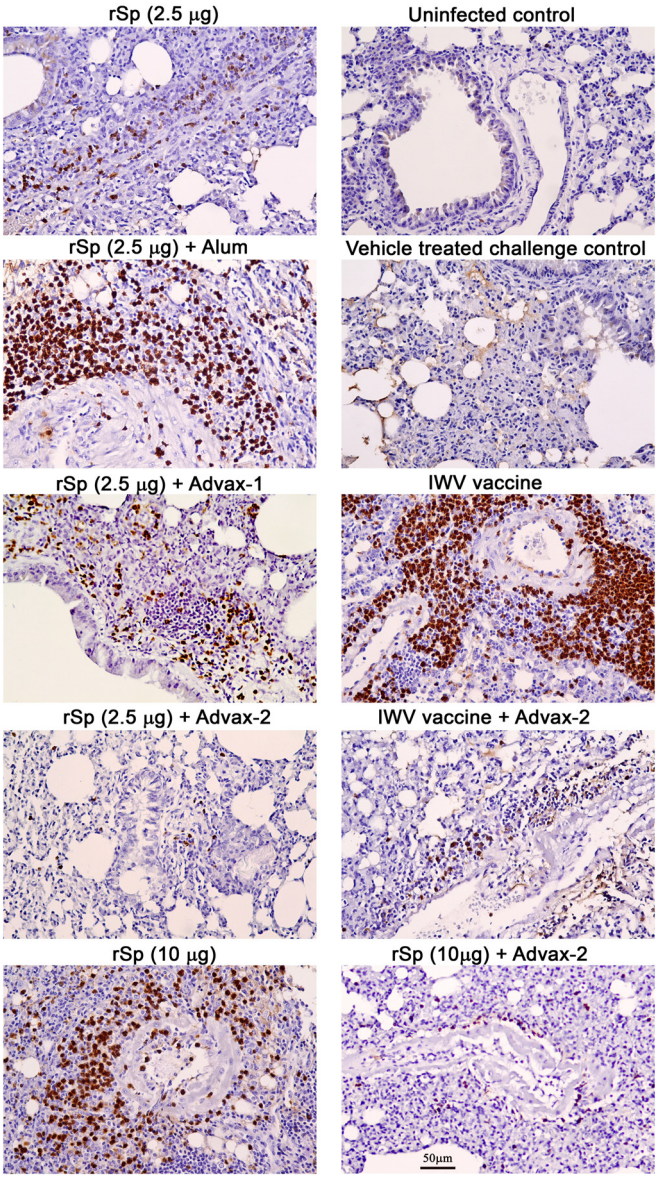

FIG 6 Lung eosinophil infiltration on day 6 postchallenge. The lungs of immunized mice from each group with the highest eosinophil infiltration scores on H&E staining on day 6 postchallenge were stained with a specific eosinophil MBP antibody (brown color).

mulated with alum protected against mortality, these mice developed severe lung eosinophilia at day 6 postchallenge (Fig. 6), reminiscent of the lung pathology induced by alum-adjuvanted RSV vaccines (20) and indicating alum's general lack of suitability as a coronavirus vaccine adjuvant. At the other end of the spectrum, mice immunized with rSP or IWV combined with Advax-2 demonstrated a complete absence of eosinophilic immunopathology (Fig. 6). The combination of rSP with Advax-2 adjuvant could thereby make an ideal coronavirus vaccine, combining the highest virus protection with the lowest risk for eosinophilic immunopathology. A surprising feature of T cells from mice immunized with Advax-2 was their lack of SP-stimulated proliferation despite high levels of IFN-γ production, a consistent feature at both 2 weeks and 1 year postimmunization. We hypothesize that this is because Advax-2 specifically induced a population of SP-specific effector memory T cells (Tem). In contrast to central memory T cells (Tcm), which are capable of self-renewal through high basal and cytokine-induced STAT5 phosphorylation, Tem cells, while retaining potent cytokine secretory ability, have largely lost the ability to proliferate in response to antigen restimulation (35–37). This lack of SP-stimulated T-cell proliferation, which was also seen in the CpG-adjuvanted group, was associated with reduced SP-stimulated IL-2 production, thereby explaining the loss of SP-stimulated proliferation. Another successful formulation was rSP plus Advax-1, with long-term immunogenicity studies showing that Advax-1 induced the most robust and durable SP-specific CD4 and CD8 T-cell response, extending out to at least 1 year postimmunization, in marked contract to the short-lived T-cell responses induced by Advax-2 or CpG. We thereby hypothesize that Advax-1 uniquely induced a long-lived SP-specific Tcm population, consistent with the high levels of SP-induced IL-2 production seen in this group at both 2 weeks and 1 year postimmunization. Thus, it is theoretically possible the Advax-1 formulation might provide the most durable coronavirus protection, a possibility that will require testing in long-term challenge studies.

How do Advax adjuvants enhance coronavirus vaccine protection? Innate immune activators such as CpG have been shown to provide short-term nonspecific virus protection via induction of interferon and other antiviral inflammatory mediators (38). However, Advax-1 or Advax-2 alone without antigen provided no protection, confirming protection to be antigen dependent. While neutralizing antibodies can provide SARS-CoV protection (39), the immunized mice had undetectable serum neutralizing antibody immediately prechallenge. Thus, the enhanced protection cannot be explained by higher levels of preexisting serum neutralizing antibody. Nevertheless, mice that received Advax-adjuvanted vaccines had significantly higher neutralizing titers as early as day 3 postchallenge, suggesting that they had preexistent memory B cells that were able to extremely rapidly produce neutralizing antibody upon virus exposure. This is supported by the finding that prechallenge, mice that had been immunized with rSP plus Advax-1 or Advax-2 had 2- to 3-fold more SP-specific bone marrow ASC than mice immunized with rSP alone. A similar mechanism whereby an expanded population of memory B cells rather than preformed serum neutralizing antibody provided enhanced viral protection by Advax-adjuvanted vaccines has recently been demonstrated in a model of Japanese encephalitis virus (26) and West Nile virus (27) infection, suggesting that memory B-cell enhancement may be a generalizable property of delta inulin adjuvants.

Enhanced protection may, however, also reflect enhancement of T-cell immunity by Advax adjuvants. SARS-CoV protection has been shown to involve coordinated action of memory CD4 and CD8 T cells together with neutralizing antibody (40). Delta inulin adjuvants have previously been shown to enhance the frequency of antigen-specific Th1, Th2, and Th17 CD4 and CD8 memory T cells in influenza (25) and hepatitis B (28) vaccine models. Most adjuvants typically bias toward particular T-cell responses, e.g., IL-4-secreting Th2 cells by alum (41), IFN-γ-secreting Th1 cells by CpG (42), and IL-17-secreting Th17 cells by oil emulsions (43). The broad enhancement of all T-cell subsets by Advax-1 is therefore unusual. Another surprise was that mice immunized with Advax-1 produced only SP-specific IgG1, a Th2 isotype, despite having large numbers of SP-specific IFN-γ-secret-

ing T cells. We hypothesize that the majority of Th1 cells in these mice might have been generated too late in the vaccine response to affect the SP-specific B-cell phenotype. In contrast, Advax-2 imparted a distinct Th1 and Th17 bias on the cellular response, with suppression of IL-4 alongside increased IFN-γ- and IL-17-secreting T cells. Surprisingly, despite the suppressed IL-4, these mice still demonstrated enhanced production of IgG1 in addition to IgG2 and IgG3. Yet another surprise was that although mice immunized with Advax-1 had enhanced T-cell IL-4 responses and solely a Th2-type antibody response, they did not develop lung eosinophilic immunopathology, in contrast to the alum-immunized mice in this and other studies (32). This raises the question of the mechanism of SARS-CoV eosinophilic immunopathology. The excess host innate immune response contributing to SARS-CoV lung pathology is complex, with roles played by alternatively activated macrophages, neutrophils, NF-κB activation, and IL-1β, IL-6, and TNF production, at least some of which reflects inflammasome activation by the envelope protein encoded ion channel (44–49). SARS-CoV lung pathology was prevented by pretreatment of alveolar macrophages with poly(I·C), a Toll-like receptor 3 (TLR3) agonist thought to act via inhibition of the excess Th2 response (50). Interestingly, Advax-1, despite increasing the frequency of IL-4-secreting SP-specific T cells, did not exacerbate eosinophilic immunopathology. The common factor between Advax-1 and Advax-2 is that they both induced SP-specific T-cell IFN-γ responses. Hence, it may be an inadequate vaccine-induced Th1 response rather than an excessive Th2 response *per se* that causes SARS-CoV lung immunopathology. This is consistent with human autopsy data showing downregulation of Th1 pathway members, STAT1, interferon, and CXCL10 in the lungs of patients who died from SARS (51). We therefore propose a model whereby immunization with SARS antigens alone or formulated with alum fails to induce a sufficient number of IFN-γ-secreting memory T cells and this lack of IFN-γ is then further exacerbated by active Th1 pathway downregulation by the SARS-CoV itself (52). This enables a vicious cycle of ever-increasing Th2-polarization of the anticoronavirus response to become established. Hence, the ideal coronavirus vaccine needs to induce not only neutralizing antibodies or, as shown here, at a minimum memory B cells capable of rapidly producing neutralizing antibody upon virus exposure but also a robust long-lived T-cell IFN-γ response, thereby preventing any risk of lung eosinophilic immunopathology. Notably, this is precisely the vaccine phenotype imparted by formulation of SARS-CoV antigens with delta inulin adjuvants.

CpG adjuvant suppressed long-term SP-specific T- and B-cell memory responses, despite providing short-term enhancement of IgG2 and IgG3 production and T-cell IFN-γ. This result is seemingly at odds with the many reports of CpG having a positive effect on humoral and cellular immunity (33). However, short-term studies of CpG could have missed a deleterious effect on long-term memory. While TLR agonists, including lipopolysaccharide, poly(U), or poly(I·C), when formulated with IWV prevented eosinophilic immunopathology (53), it will be important to make sure that such protective effects do not wane over time. The mechanism underlying the suppression of long-term T-cell memory by CpG observed here is currently unknown; we hypothesize that it reflects induction by CpG of short-lived effector T cells that in the absence of IL-2 rapidly die once the initial vaccine stimulus wanes.

Important questions remain to be addressed, including identification of the best strategies to protect elderly subjects, the population most vulnerable to lethal human coronaviruses. There is also the important issue of how best to provide protection against variant and heterologous coronavirus strains. While this study did not address these questions directly, Advax adjuvants have previously been shown to enhance human vaccine responses in elderly subjects (30) and provided enhanced heterologous protection against West Nile virus in mice immunized with an inactivated Japanese encephalitis virus antigen (27). Hence, it will be interesting to see whether delta inulin adjuvants can similarly enhance heterologous coronavirus protection, including in elderly mouse models. Future studies are also needed to test the longevity of SARS-CoV vaccine protection achievable with the different adjuvant formulations, and it will also be important to extend the current findings to larger animals such as the ferret SARS-CoV model.

In conclusion, this study highlights the critical importance of adjuvant selection for development of effective and safe coronavirus vaccines. Delta inulin-based adjuvants were shown here for the first time to provide enhance humoral and T-cell responses to both recombinant and inactivated whole-virus SARS-CoV antigens, boosting vaccine protection while avoiding the risk of lung immunopathology. These findings should assist the design of optimal vaccines against SARS-CoV, MERS-CoV, and other potential human coronavirus threats.

ACKNOWLEDGMENTS

We thank Anna Lalusis-Derks, Marco Meier, Robb Muirhead, Samay Trec, Connie Li, and Annasaheb Kolpe for technical assistance. We thank Fred Cassels for assistance with arranging the SARS-CoV challenge studies. The following reagents were obtained through the NIH Biodefense and Emerging Infections Research Resources Repository, NIAID, NIH: formaldehyde- and UV-inactivated, purified SARS-CoV vaccine NR-3882; SARS-CoV spike protein NR-722; β-propiolactone-inactivated, alum-adsorbed SARS-CoV NR-9599; and formaldehyde-and UV inactivated SARS-CoV NR-9724.

This project has been funded in part with Federal funds from the National Institute of Allergy and Infectious Diseases, National Institutes of Health, Department of Health and Human Services, under contract no. HHSN272200800039C and collaborative research contact no. U01AI061142 to Vaxine Pty Ltd. and contracts HHSN272201000039I and HHSN27200002/A14 to Utah State University.

The content is solely the responsibility of the authors, and the funders played no role in the writing of the manuscript.

REFERENCES

1. **Drosten C, Gunther S, Preiser W, van der Werf S, Brodt HR, Becker S, Rabenau H, Panning M, Kolesnikova L, Fouchier RA, Berger A, Burguiere AM, Cinatl J, Eickmann M, Escriou N, Grywna K, Kramme S, Manuguerra JC, Muller S, Rickerts V, Sturmer M, Vieth S, Klenk HD, Osterhaus AD, Schmitz H, Doerr HW.** 2003. Identification of a novel coronavirus in patients with severe acute respiratory syndrome. N Engl J Med **348:**1967–1976. http://dx.doi.org/10.1056/NEJMoa030747.
2. **Rota PA, Oberste MS, Monroe SS, Nix WA, Campagnoli R, Icenogle JP, Penaranda S, Bankamp B, Maher K, Chen MH, Tong S, Tamin A, Lowe L, Frace M, DeRisi JL, Chen Q, Wang D, Erdman DD, Peret TC, Burns C, Ksiazek TG, Rollin PE, Sanchez A, Liffick S, Holloway B, Limor J, McCaustland K, Olsen-Rasmussen M, Fouchier R, Gunther S, Osterhaus AD, Drosten C, Pallansch MA, Anderson LJ, Bellini WJ.** 2003. Characterization of a novel coronavirus associated with severe acute respiratory syndrome. Science **300:**1394–1399. http://dx.doi.org/10.1126/science.1085952.
3. **Nicholls J, Dong XP, Jiang G, Peiris M.** 2003. SARS: clinical virology and pathogenesis. Respirology **8**(Suppl)**:**S6–S8. http://dx.doi.org/10.1046/j.1440-1843.2003.00517.x.

4. **Graham RL, Donaldson EF, Baric RS.** 2013. A decade after SARS: strategies for controlling emerging coronaviruses. Nat Rev Microbiol **11:**836–848. http://dx.doi.org/10.1038/nrmicro3143.
5. **Callow KA, Parry HF, Sergeant M, Tyrrell DA.** 1990. The time course of the immune response to experimental coronavirus infection of man. Epidemiol Infect **105:**435–446. http://dx.doi.org/10.1017/S0950268800048019.
6. **Tang F, Quan Y, Xin ZT, Wrammert J, Ma MJ, Lv H, Wang TB, Yang H, Richardus JH, Liu W, Cao WC.** 2011. Lack of peripheral memory B cell responses in recovered patients with severe acute respiratory syndrome: a six-year follow-up study. J Immunol **186:**7264–7268. http://dx.doi.org/10.4049/jimmunol.0903490.
7. **Wang SF, Tseng SP, Yen CH, Yang JY, Tsao CH, Shen CW, Chen KH, Liu FT, Liu WT, Chen YM, Huang JC.** 2014. Antibody-dependent SARS coronavirus infection is mediated by antibodies against spike proteins. Biochem Biophys Res Commun **451:**208–214. http://dx.doi.org/10.1016/j.bbrc.2014.07.090.
8. **Assiri A, McGeer A, Perl TM, Price CS, Al Rabeeah AA, Cummings DA, Alabdullatif ZN, Assad M, Almulhim A, Makhdoom H, Madani H, Alhakeem R, Al-Tawfiq JA, Cotten M, Watson SJ, Kellam P, Zumla AI, Memish ZA.** 2013. Hospital outbreak of Middle East respiratory syndrome coronavirus. N Engl J Med **369:**407–416. http://dx.doi.org/10.1056/NEJMoa1306742.
9. **Marra MA, Jones SJ, Astell CR, Holt RA, Brooks-Wilson A, Butterfield YS, Khattra J, Asano JK, Barber SA, Chan SY, Cloutier A, Coughlin SM, Freeman D, Girn N, Griffith OL, Leach SR, Mayo M, McDonald H, Montgomery SB, Pandoh PK, Petrescu AS, Robertson AG, Schein JE, Siddiqui A, Smailus DE, Stott JM, Yang GS, Plummer F, Andonov A, Artsob H, Bastien N, Bernard K, Booth TF, Bowness D, Czub M, Drebot M, Fernando L, Flick R, Garbutt M, Gray M, Grolla A, Jones S, Feldmann H, Meyers A, Kabani A, Li Y, Normand S, Stroher U, Tipples GA, Tyler S, et al.** 2003. The genome sequence of the SARS-associated coronavirus. Science **300:**1399–1404. http://dx.doi.org/10.1126/science.1085953.
10. **Darnell ME, Plant EP, Watanabe H, Byrum R, St Claire M, Ward JM, Taylor DR.** 2007. Severe acute respiratory syndrome coronavirus infection in vaccinated ferrets. J Infect Dis **196:**1329–1338. http://dx.doi.org/10.1086/522431.
11. **Bolles M, Deming D, Long K, Agnihothram S, Whitmore A, Ferris M, Funkhouser W, Gralinski L, Totura A, Heise M, Baric RS.** 2011. A double-inactivated severe acute respiratory syndrome coronavirus vaccine provides incomplete protection in mice and induces increased eosinophilic proinflammatory pulmonary response upon challenge. J Virol **85:**12201–12215. http://dx.doi.org/10.1128/JVI.06048-11.
12. **See RH, Zakhartchouk AN, Petric M, Lawrence DJ, Mok CP, Hogan RJ, Rowe T, Zitzow LA, Karunakaran KP, Hitt MM, Graham FL, Prevec L, Mahony JB, Sharon C, Auperin TC, Rini JM, Tingle AJ, Scheifele DW, Skowronski DM, Patrick DM, Voss TG, Babiuk LA, Gauldie J, Roper RL, Brunham RC, Finlay BB.** 2006. Comparative evaluation of two severe acute respiratory syndrome (SARS) vaccine candidates in mice challenged with SARS coronavirus. J Gen Virol **87:**641–650. http://dx.doi.org/10.1099/vir.0.81579-0.
13. **Yasui F, Kai C, Kitabatake M, Inoue S, Yoneda M, Yokochi S, Kase R, Sekiguchi S, Morita K, Hishima T, Suzuki H, Karamatsu K, Yasutomi Y, Shida H, Kidokoro M, Mizuno K, Matsushima K, Kohara M.** 2008. Prior immunization with severe acute respiratory syndrome (SARS)-associated coronavirus (SARS-CoV) nucleocapsid protein causes severe pneumonia in mice infected with SARS-CoV. J Immunol **181:**6337–6348. http://dx.doi.org/10.4049/jimmunol.181.9.6337.
14. **Tseng CT, Sbrana E, Iwata-Yoshikawa N, Newman PC, Garron T, Atmar RL, Peters CJ, Couch RB.** 2012. Immunization with SARS coronavirus vaccines leads to pulmonary immunopathology on challenge with the SARS virus. PLoS One **7:**e35421. http://dx.doi.org/10.1371/journal.pone.0035421.
15. **Clay C, Donart N, Fomukong N, Knight JB, Lei W, Price L, Hahn F, Van Westrienen J, Harrod KS.** 2012. Primary severe acute respiratory syndrome coronavirus infection limits replication but not lung inflammation upon homologous rechallenge. J Virol **86:**4234–4244. http://dx.doi.org/10.1128/JVI.06791-11.
16. **Li W, Moore MJ, Vasilieva N, Sui J, Wong SK, Berne MA, Somasundaran M, Sullivan JL, Luzuriaga K, Greenough TC, Choe H, Farzan M.** 2003. Angiotensin-converting enzyme 2 is a functional receptor for the SARS coronavirus. Nature **426:**450–454. http://dx.doi.org/10.1038/nature02145.
17. **Jeffers SA, Tusell SM, Gillim-Ross L, Hemmila EM, Achenbach JE, Babcock GJ, Thomas WD, Jr, Thackray LB, Young MD, Mason RJ, Ambrosino DM, Wentworth DE, Demartini JC, Holmes KV.** 2004. CD209L (L-SIGN) is a receptor for severe acute respiratory syndrome coronavirus. Proc Natl Acad Sci U S A **101:**15748–15753. http://dx.doi.org/10.1073/pnas.0403812101.
18. **Huang J, Cao Y, Du J, Bu X, Ma R, Wu C.** 2007. Priming with SARS CoV S DNA and boosting with SARS CoV S epitopes specific for CD4+ and CD8+ T cells promote cellular immune responses. Vaccine **25:**6981–6991. http://dx.doi.org/10.1016/j.vaccine.2007.06.047.
19. **Zhou Z, Post P, Chubet R, Holtz K, McPherson C, Petric M, Cox M.** 2006. A recombinant baculovirus-expressed S glycoprotein vaccine elicits high titers of SARS-associated coronavirus (SARS-CoV) neutralizing antibodies in mice. Vaccine **24:**3624–3631. http://dx.doi.org/10.1016/j.vaccine.2006.01.059.
20. **Openshaw PJ, Culley FJ, Olszewska W.** 2001. Immunopathogenesis of vaccine-enhanced RSV disease. Vaccine **20**(Suppl 1)**:**S27–S31. http://dx.doi.org/10.1016/S0264-410X(01)00301-2.
21. **Petrovsky N, Aguilar JC.** 2004. Vaccine adjuvants: current state and future trends. Immunol Cell Biol **82:**488–496. http://dx.doi.org/10.1111/j.0818-9641.2004.01272.x.
22. **Petrovsky N, Cooper PD.** 2011. Carbohydrate-based immune adjuvants. Expert Rev Vaccines **10:**523–537. http://dx.doi.org/10.1586/erv.11.30.
23. **Cooper PD, Petrovsky N.** 2011. Delta inulin: a novel, immunologically active, stable packing structure comprising beta-D-[2→1]poly(fructofuranosyl)alpha-D-glucose polymers. Glycobiology **21:**595–606. http://dx.doi.org/10.1093/glycob/cwq201.
24. **Layton RC, Petrovsky N, Gigliotti AP, Pollock Z, Knight J, Donart N, Pyles J, Harrod KS, Gao P, Koster F.** 2011. Delta inulin polysaccharide adjuvant enhances the ability of split-virion H5N1 vaccine to protect against lethal challenge in ferrets. Vaccine **29:**6242–6251. http://dx.doi.org/10.1016/j.vaccine.2011.06.078.
25. **Honda-Okubo Y, Saade F, Petrovsky N.** 2012. Advax, a polysaccharide adjuvant derived from delta inulin, provides improved influenza vaccine protection through broad-based enhancement of adaptive immune responses. Vaccine **30:**5373–5381. http://dx.doi.org/10.1016/j.vaccine.2012.06.021.
26. **Larena M, Prow NA, Hall RA, Petrovsky N, Lobigs M.** 2013. JE-ADVAX vaccine protection against Japanese encephalitis virus mediated by memory B cells in the absence of CD8+ T cells and preexposure neutralizing antibody. J Virol **87:**4395–4402. http://dx.doi.org/10.1128/JVI.03144-12.
27. **Petrovsky N, Larena M, Siddharthan V, Prow NA, Hall RA, Lobigs M, Morrey J.** 2013. An inactivated cell culture Japanese encephalitis vaccine (JE-ADVAX) formulated with delta inulin adjuvant provides robust heterologous protection against West Nile encephalitis via cross-protective memory B cells and neutralizing antibody. J Virol **87:**10324–10333. http://dx.doi.org/10.1128/JVI.00480-13.
28. **Saade F, Honda-Okubo Y, Trec S, Petrovsky N.** 2013. A novel hepatitis B vaccine containing Advax, a polysaccharide adjuvant derived from delta inulin, induces robust humoral and cellular immunity with minimal reactogenicity in preclinical testing. Vaccine **31:**1999–2007. http://dx.doi.org/10.1016/j.vaccine.2012.12.077.
29. **Cristillo AD, Ferrari MG, Hudacik L, Lewis B, Galmin L, Bowen B, Thompson D, Petrovsky N, Markham P, Pal R.** 2011. Induction of mucosal and systemic antibody and T-cell responses following prime-boost immunization with novel adjuvanted human immunodeficiency virus-1-vaccine formulations. J Gen Virol **92:**128–140. http://dx.doi.org/10.1099/vir.0.023242-0.
30. **Gordon DL, Sajkov D, Woodman RJ, Honda-Okubo Y, Cox MM, Heinzel S, Petrovsky N.** 2012. Randomized clinical trial of immunogenicity and safety of a recombinant H1N1/2009 pandemic influenza vaccine containing Advax polysaccharide adjuvant. Vaccine **30:**5407–5416. http://dx.doi.org/10.1016/j.vaccine.2012.06.009.
31. **Gordon D, Kelley P, Heinzel S, Cooper P, Petrovsky N.** 27 September 2014. Immunogenicity and safety of Advax, a novel polysaccharide adjuvant based on delta inulin, when formulated with hepatitis B surface antigen: a randomized controlled phase 1 study. Vaccine http://dx.doi.org/10.1016/j.vaccine.2014.09.034.
32. **Day CW, Baric R, Cai SX, Frieman M, Kumaki Y, Morrey JD, Smee DF, Barnard DL.** 2009. A new mouse-adapted strain of SARS-CoV as a lethal

model for evaluating antiviral agents in vitro and in vivo. Virology **395:** 210–222. http://dx.doi.org/10.1016/j.virol.2009.09.023.
33. **Chu RS, Targoni OS, Krieg AM, Lehmann PV, Harding CV.** 1997. CpG oligodeoxynucleotides act as adjuvants that switch on T helper 1 (Th1) immunity. J Exp Med **186:**1623–1631. http://dx.doi.org/10.1084/jem.186.10.1623.
34. **Ma C, Wang L, Tao X, Zhang N, Yang Y, Tseng CT, Li F, Zhou Y, Jiang S, Du L.** 2014. Searching for an ideal vaccine candidate among different MERS coronavirus receptor-binding fragments—the importance of immunofocusing in subunit vaccine design. Vaccine **32:**6170–6176. http://dx.doi.org/10.1016/j.vaccine.2014.08.086.
35. **Willinger T, Freeman T, Hasegawa H, McMichael AJ, Callan MF.** 2005. Molecular signatures distinguish human central memory from effector memory CD8 T cell subsets. J Immunol **175:**5895–5903. http://dx.doi.org/10.4049/jimmunol.175.9.5895.
36. **Geginat J, Lanzavecchia A, Sallusto F.** 2003. Proliferation and differentiation potential of human CD8+ memory T-cell subsets in response to antigen or homeostatic cytokines. Blood **101:**4260–4266. http://dx.doi.org/10.1182/blood-2002-11-3577.
37. **Sallusto F, Lenig D, Forster R, Lipp M, Lanzavecchia A.** 1999. Two subsets of memory T lymphocytes with distinct homing potentials and effector functions. Nature **401:**708–712. http://dx.doi.org/10.1038/44385.
38. **Wong JP, Christopher ME, Viswanathan S, Karpoff N, Dai X, Das D, Sun LQ, Wang M, Salazar AM.** 2009. Activation of Toll-like receptor signaling pathway for protection against influenza virus infection. Vaccine **27:**3481–3483. http://dx.doi.org/10.1016/j.vaccine.2009.01.048.
39. **Berger A, Drosten C, Doerr HW, Sturmer M, Preiser W.** 2004. Severe acute respiratory syndrome (SARS)—paradigm of an emerging viral infection. J Clin Virol **29:**13–22. http://dx.doi.org/10.1016/j.jcv.2003.09.011.
40. **Channappanavar R, Fett C, Zhao J, Meyerholz DK, Perlman S.** 2014. Virus-specific memory CD8 T cells provide substantial protection from lethal severe acute respiratory syndrome coronavirus infection. J Virol **88:**11034–11044. http://dx.doi.org/10.1128/JVI.01505-14.
41. **Terhune TD, Deth RC.** 2013. How aluminum adjuvants could promote and enhance non-target IgE synthesis in a genetically-vulnerable subpopulation. J Immunotoxicol **10:**210–222. http://dx.doi.org/10.3109/1547691X.2012.708366.
42. **Brazolot Millan CL, Weeratna R, Krieg AM, Siegrist CA, Davis HL.** 1998. CpG DNA can induce strong Th1 humoral and cell-mediated immune responses against hepatitis B surface antigen in young mice. Proc Natl Acad Sci U S A **95:**15553–15558. http://dx.doi.org/10.1073/pnas.95.26.15553.
43. **Zhao J, Lloyd CM, Noble A.** 2013. Th17 responses in chronic allergic airway inflammation abrogate regulatory T-cell-mediated tolerance and contribute to airway remodeling. Mucosal Immunol **6:**335–346. http://dx.doi.org/10.1038/mi.2012.76.
44. **Fett C, DeDiego ML, Regla-Nava JA, Enjuanes L, Perlman S.** 2013. Complete protection against severe acute respiratory syndrome coronavirus-mediated lethal respiratory disease in aged mice by immunization with a mouse-adapted virus lacking E protein. J Virol **87:**6551–6559. http://dx.doi.org/10.1128/JVI.00087-13.
45. **Nieto-Torres JL, DeDiego ML, Verdia-Baguena C, Jimenez-Guardeno JM, Regla-Nava JA, Fernandez-Delgado R, Castano-Rodriguez C, Alcaraz A, Torres J, Aguilella VM, Enjuanes L.** 2014. Severe acute respiratory syndrome coronavirus envelope protein ion channel activity promotes virus fitness and pathogenesis. PLoS Pathog **10:**e1004077. http://dx.doi.org/10.1371/journal.ppat.1004077.
46. **Smits SL, van den Brand JM, de Lang A, Leijten LM, van Ijcken WF, van Amerongen G, Osterhaus AD, Andeweg AC, Haagmans BL.** 2011. Distinct severe acute respiratory syndrome coronavirus-induced acute lung injury pathways in two different nonhuman primate species. J Virol **85:**4234–4245. http://dx.doi.org/10.1128/JVI.02395-10.
47. **Rockx B, Baas T, Zornetzer GA, Haagmans B, Sheahan T, Frieman M, Dyer MD, Teal TH, Proll S, van den Brand J, Baric R, Katze MG.** 2009. Early upregulation of acute respiratory distress syndrome-associated cytokines promotes lethal disease in an aged-mouse model of severe acute respiratory syndrome coronavirus infection. J Virol **83:**7062–7074. http://dx.doi.org/10.1128/JVI.00127-09.
48. **Page C, Goicochea L, Matthews K, Zhang Y, Klover P, Holtzman MJ, Hennighausen L, Frieman M.** 2012. Induction of alternatively activated macrophages enhances pathogenesis during severe acute respiratory syndrome coronavirus infection. J Virol **86:**13334–13349. http://dx.doi.org/10.1128/JVI.01689-12.
49. **DeDiego ML, Nieto-Torres JL, Regla-Nava JA, Jimenez-Guardeno JM, Fernandez-Delgado R, Fett C, Castano-Rodriguez C, Perlman S, Enjuanes L.** 2014. Inhibition of NF-kappaB-mediated inflammation in severe acute respiratory syndrome coronavirus-infected mice increases survival. J Virol **88:**913–924. http://dx.doi.org/10.1128/JVI.02576-13.
50. **Zhao J, Wohlford-Lenane C, Zhao J, Fleming E, Lane TE, McCray PB, Jr, Perlman S.** 2012. Intranasal treatment with poly(I*C) protects aged mice from lethal respiratory virus infections. J Virol **86:**11416–11424. http://dx.doi.org/10.1128/JVI.01410-12.
51. **Kong SL, Chui P, Lim B, Salto-Tellez M.** 2009. Elucidating the molecular physiopathology of acute respiratory distress syndrome in severe acute respiratory syndrome patients. Virus Res **145:**260–269. http://dx.doi.org/10.1016/j.virusres.2009.07.014.
52. **Yoshikawa T, Hill T, Li K, Peters CJ, Tseng CT.** 2009. Severe acute respiratory syndrome (SARS) coronavirus-induced lung epithelial cytokines exacerbate SARS pathogenesis by modulating intrinsic functions of monocyte-derived macrophages and dendritic cells. J Virol **83:**3039–3048. http://dx.doi.org/10.1128/JVI.01792-08.
53. **Iwata-Yoshikawa N, Uda A, Suzuki T, Tsunetsugu-Yokota Y, Sato Y, Morikawa S, Tashiro M, Sata T, Hasegawa H, Nagata N.** 2014. Effects of Toll-like receptor stimulation on eosinophilic infiltration in lungs of BALB/c mice immunized with UV-inactivated severe acute respiratory syndrome-related coronavirus vaccine. J Virol **88:**8597–8614. http://dx.doi.org/10.1128/JVI.00983-14.